NASA Contractor Report 165990

NASA-CR-165990
19820018831

THE CRACK AND WEDGING PROBLEM FOR AN ORTHOTROPIC STRIP

A. Cinar and F. Erdogan

LEHIGH UNIVERSITY
Bethlehem, Pennsylvania 18015

Grant NGR 39-007-011
September 1982

National Aeronautics and
Space Administration

Langley Research Center
Hampton, Virginia 23665

THE CRACK AND WEDGING PROBLEM FOR AN ORTHOTROPIC STRIP(*)

A. Cinar and F. Erdogan
Lehigh University, Bethlehem, PA

ABSTRACT

In this paper first the plane elasticity problem for an orthotropic strip containing a crack parallel to its boundaries is considered. The problem is formulated under general mixed mode loading conditions. It is shown that the stress intensity factors depend on two dimensionless orthotropic constants only. For the crack problem the results are given for a single crack and two collinear cracks. The calculated results show that of the two orthotropic constants the influence of the stiffness ratio on the stress intensity factors is much more significant than that of the shear parameter. The problem of loading the strip by a rigid rectangular wedge is then considered. It is found that for relatively small wedge lengths continuous contact is maintained along the wedge-strip interface, at a certain critical wedge length the separation starts at the midsection of the wedge, and the length of the separation zone increases rapidly with increasing wedge length.

1. Introduction

From the plane elasticity solution of an infinite orthotropic medium containing a series of collinear cracks it is known that the material orthotropy has no effect on the stress intensity factors [1] (see also [2] and [3] for the case of a single crack). On the other hand, the solution given for an infinite strip has shown that if the medium is bounded then the stress intensity factors would be influenced by the material orthotropy [4,5]. If the (collinear) cracks are perpendicular to the boundaries of the strip and if the external loads are independent of the coordinate parallel to the boundaries, then the stress intensity

(*)This work was supported by NASA-Langley under the Grant NGR 39-007-011.

factors and indeed the stress component in the plane of the cracks turn out to be invariant with regard to a 90-degree material rotation [4]. This result is not valid if the strip is loaded along its boundaries (e.g., bending of the strip by transverse shear loads) [5]. Even though there exists a general solution for an orthotropic strip containing an inclined crack [6], a systematic solution of an orthotropic strip containing cracks parallel to its boundaries investigating such factors as the relative size and location of the crack, the types of loading, and the material constants does not seem to exist in literature. Such a problem would have applications to, for example, the study of delamination fracture in layered composites, wood and other homogeneous orthotropic solids.

In this paper, first the general problem of an orthotropic strip containing a crack located at an arbitrary distance from and oriented parallel to the boundaries is considered. The effect of interaction of more than one crack on the stress intenstiy factors is studied by considering two collinear cracks in the strip. The important problem of splitting the strip by a rigid wedge is then investigated. For a wedge of rectangular cross-section which is short relative to the crack length it is shown that the wedge remains in contact with the strip along its entire length. However, for wedges longer than a critical length the contact is shown to be restricted near the ends of the wedge only. It is also shown that neither the critical wedge length nor the length of the contact region is dependent on the wedge thickness.

2. Formulation of the Crack Problem

Defining a stress function ϕ by

$$\sigma_{11} = \frac{\partial^2 \phi}{\partial x_2^2}, \quad \sigma_{22} = \frac{\partial^2 \phi}{\partial x_1^2}, \quad \sigma_{12} = -\frac{\partial^2 \phi}{\partial x_1 \partial x_2}, \tag{1}$$

the compatibility condition for the generalized plane stress problem for an orthotropic plate may be expressed as [7]

$$\frac{E_{11}}{E_{22}}\frac{\partial^4\phi}{\partial x_1^4} + \left(\frac{E_{11}}{G_{12}} - 2\nu_{12}\right)\frac{\partial^4\phi}{\partial x_1^2\partial x_2^2} + \frac{\partial^4\phi}{\partial x_2^4} = 0 \quad , \tag{2}$$

where the notation for the engineering material constants is given by the following stress-strain relations:

$$\varepsilon_{11} = \frac{1}{E_{11}}(\sigma_{11} - \nu_{12}\sigma_{22} - \nu_{13}\sigma_{33}) \ , \ \cdots \ ,$$

$$2\varepsilon_{12} = \frac{1}{G_{12}}\sigma_{12} \ , \ \cdots \tag{3}$$

For the plane stress problem introducing [8]

$$E = \sqrt{E_{11}E_{22}} \ , \quad \nu = \sqrt{\nu_{12}\nu_{21}} \ , \quad \delta^4 = E_{11}/E_{22} \ , \ \kappa = \frac{E}{2G_{12}} - \nu \ , \tag{4}$$

and defining

$$x = \frac{x_1}{\sqrt{\delta}} \ , \ y = x_2\sqrt{\delta} \ , \ \sigma_{xx} = \sigma_{11}/\delta, \ \sigma_{yy} = \delta\sigma_{22} \ , \ \sigma_{xy} = \sigma_{12} \tag{5}$$

from (1) and (2) it follows that

$$\sigma_{xx} = \frac{\partial^2\phi}{\partial y^2} \ , \ \sigma_{yy} = \frac{\partial^2\phi}{\partial x^2} \ , \ \sigma_{xy} = -\frac{\partial^2\phi}{\partial x\partial y} \ , \tag{6}$$

$$\frac{\partial^4\phi}{\partial x^4} + 2\kappa\frac{\partial^4\phi}{\partial x^2\partial y^2} + \frac{\partial^4\phi}{\partial y^4} = 0 \quad . \tag{7}$$

It may easily be verified that with the transformation (5) equations (6) and (7) remain valid for the plane strain case provided the stiffness ratio δ and the shear parameter κ are defined as follows [8]:

$$\delta^4 = \frac{E_{11}}{E_{22}}\frac{1-\nu_{23}\nu_{32}}{1-\nu_{13}\nu_{31}} \ ,$$

$$\kappa = \frac{1}{2}\left[\frac{E_{11}E_{22}}{(1-\nu_{13}\nu_{31})(1-\nu_{23}\nu_{32})}\right]^{1/2}\left(\frac{1}{G_{12}} - \frac{\nu_{21}+\nu_{23}\nu_{31}}{E_{22}} - \frac{\nu_{12}+\nu_{13}\nu_{32}}{E_{11}}\right) \ . \tag{8}$$

In this case the effective stiffness E and the effective Poisson's ratio ν are defined by

$$E = \left[\frac{E_{11}E_{22}}{(1-\nu_{13}\nu_{31})(1-\nu_{23}\nu_{32})}\right]^{1/2},$$

$$\nu = \left[\frac{(\nu_{12}+\nu_{13}\nu_{32})(\nu_{21}+\nu_{23}\nu_{31})}{(1-\nu_{13}\nu_{31})(1-\nu_{23}\nu_{32})}\right]^{1/2}. \tag{9}$$

Also introducing the new displacements by

$$u = u_1\sqrt{\delta}\ ,\ v = u_2/\sqrt{\delta}\ , \tag{10}$$

The strains and the stress-strain relations may be written as follows:

$$\varepsilon_{xx} = \delta\varepsilon_{11} = \frac{\partial u}{\partial x}\ ,\ \varepsilon_{yy} = \frac{\varepsilon_{22}}{\delta} = \frac{\partial v}{\partial y}\ ,\ \varepsilon_{xy} = \varepsilon_{12} = (\frac{\partial u}{\partial y} + \frac{\partial v}{\partial x})/2, \tag{11}$$

$$\varepsilon_{xx} = \frac{1}{E}(\sigma_{xx}-\nu\sigma_{yy})\ ,\ \varepsilon_{yy} = \frac{1}{E}(\sigma_{yy}-\nu\sigma_{xx}),\ \varepsilon_{xy} = \frac{(\kappa+\nu)}{E}\sigma_{xy}\ . \tag{12}$$

For the strip shown in Fig. 1a in terms of standard Fourier integrals the solution of the differential equation (7) may be expressed as

$$\phi(x,y) = \phi_1(x,y) + \phi_2(x,y) \tag{13}$$

$$\phi_1(x,y) = \frac{1}{2\pi}\int_{-\infty}^{\infty}\sum_{j=1}^{4} C_j(\alpha)e^{\alpha y s_j - i\alpha x}\,d\alpha\ ,\ -H_2<y/\sqrt{\delta}<H_1, \tag{14}$$

$$\begin{aligned}\phi_2(x,y) &= \frac{1}{2\pi}\int_{-\infty}^{\infty}\sum_{j=1}^{2} A_j(\alpha)e^{-|\alpha|ys_j - i\alpha x}\,d\alpha\ ,\ y>0\ ,\\ \phi_2(x,y) &= \frac{1}{2\pi}\int_{-\infty}^{\infty}\sum_{j=1}^{2} A_{j+2}(\alpha)e^{|\alpha|ys_j - i\alpha x}\,d\alpha\ ,\ y<0\end{aligned} \tag{15}$$

where $s_1,\ldots,s_4$ are the roots of

$$s^4 - 2\kappa s^2 + 1 = 0 \tag{16}$$

and are given by

$$s_1 = (\kappa+\sqrt{\kappa^2-1})^{1/2},\ s_2 = (\kappa-\sqrt{\kappa^2-1})^{1/2},\ s_3 = -s_1,\ s_4 = -s_2\ . \tag{17}$$

The functions ϕ_1 and ϕ_2 are respectively associated with a strip without any cracks and an infinite plane containing collinear cracks along the x-axis. The unknown functions C_j and A_j, $(j=1,\ldots,4)$ are determined from the following eight boundary and continuity conditions (see Fig. 1a and equations (5))

$$\sigma_{22}(x_1,H_1) = 0,\ \sigma_{12}(x_1,H_1) = 0,\ \sigma_{22}(x_1,-H_2) = 0,\ \sigma_{12}(x_1,-H_2) = 0,$$
$$-\infty < x_1 < \infty\ , \tag{18}$$

$$\sigma_{22}(x_1,+0) = \sigma_{22}(x_1,-0),\ \sigma_{12}(x_1,+0) = \sigma_{12}(x_1,-0),\ -\infty < x_1 < \infty, \tag{19}$$

$$\sigma_{22}(x_1,0) = \sigma(x_1)\ ,\ \sigma_{12}(x_1,0) = \tau(x_1)\ ,\ -a < x_1 < a\ , \tag{20}$$

$$u_2(x_1,+0)-u_2(x_1,-0) = 0,\ u_1(x_1,+0)-u_1(x_1,-0) = 0\ ,\ |x_1| > a\ . \tag{21}$$

The six homogeneous conditions (18) and (19) may be used to eliminate six of the eight unknown functions. The mixed boundary conditions (20) and (21) would then give a system of dual integral equations to determine the remaining two functions. By defining the new unknown functions

$$G_2(x_1) = \frac{\partial}{\partial x_1}[u_1(x_1,+0)-u_1(x_1,-0)],\ G_1(x_1) = \frac{\partial}{\partial x_1}[u_2(x_1,+0)-u_2(x_1,-0)] \tag{22}$$

the problem may also be reduced to a system of integral equations in G_1 and G_2. In this case it is seen that (21) is equivalent to

$$G_j(x_1) = 0, \ |x_1| > a \ , \ \int_{-a}^{a} G_j(x_1)dx_1 = 0 \ , \ (j = 1,2) \ , \tag{23}$$

and (20) gives the desired integral equations.

The displacements and stresses contributed by ϕ_1 are continuous on $x_2 = 0$ plane. Thus, the functions A_3 and A_4 are eliminated by substituting from (15) and (17) into the continuity conditions (19), giving

$$A_3 = [(s_1+s_2)A_1 + 2s_2A_2]/(s_2-s_1) \ ,$$

$$A_4 = [2s_1A_1 + (s_1+s_2)A_2]/(s_1-s_2) \ . \tag{24}$$

Substituting now from (6) and (15) through the Hooke's law into (21) and by using (22), A_1 and A_2 may be obtained in terms of the Fourier transforms of G_1 and G_2. The functions $C_1,\ldots,C_4$ are then determined from the boundary conditions (18), again in terms of the Fourier transforms of G_1 and G_2. Noting that G_1 and G_2 are zero for $|x_1|>a$, the expressions found for A_1, A_2, $C_1,\ldots,C_4$ are of the following form

$$A_j(\alpha) = \sum_{k=1}^{2} a_{jk}(\alpha) \int_{-a}^{a} G_k(t)e^{i\alpha t} \ dt \ , \ j = 1,2,$$

$$C_j(\alpha) = \sum_{k=1}^{2} c_{jk}(\alpha) \int_{-a}^{a} G_k(t)e^{i\alpha t} \ dt, \ j = 1,\ldots,4 \ , \tag{25}$$

where a_{jk} and c_{jk} are known functions. Substituting from (5), (6), (13)-(15) and (25) into the remaining boundary conditions (19) and performing a standard asymptotic analysis to separate the singular parts of the kernels we obtain the following system of integral equations to determine the unknown functions G_1 and G_2:

$$\frac{1}{\pi}\int_{-a}^{a}\left[\frac{G_1(t_1)}{t_1-x_1}+k_{11}(x_1,t_1)G_1(t_1)+k_{12}(x_1,t_1)G_2(t_1)\delta\right]dt_1$$

$$=\frac{\delta}{Em_1}\,\sigma(x_1)\ ,\ -a<x_1<a\ ,$$

$$\frac{1}{\pi}\int_{-a}^{a}\left[\frac{\delta G_2(t_1)}{t_1-x_1}+k_{21}(x_1,t_1)G_1(t_1)+k_{22}(x_1,t_1)G_2(t_1)\delta\right]dt_1$$

$$=\frac{1}{Em_2}\,\tau(x_1)\ ,\ -a<x_1<a\ , \tag{26}$$

where k_{ij} $((i,j)=(1,2))$ are known bounded functions and the constants m_1 and m_2 are given in terms of the roots s_1, s_2 (see (17)). The derivations leading to (26) as well as the expressions for the kernels k_{ij} are rather lengthy but very straightforward. Therefore, they will not be reproduced in this paper. The details of the analysis may be found in [9].

One should emphasize that the kernels k_{ij} are dependent on the shear parameter κ through the characteristic roots s_1 and s_2, the stiffness parameter δ, and the dimensions a, H_1 and H_2, $(H_1+H_2=H)$. However, the analysis shows that aside from κ the remaining variables enter into the expressions of the kernels through the ratios H_1/H_2 and $\delta H/a$ only. The solution of the system of singular integral equations is of the following form:

$$G_j(x_1)=\frac{F_j(x_1)}{(a^2-x_1^2)^{\frac{1}{2}}}\ ,\ j=1,2,\ldots \tag{27}$$

where F_1 and F_2 are bounded unknown functions. After normalizing the interval (-a,a) (26) may be solved numerically by using a Gaussian quadrature formula [10].

3. Stress Intensity Factors

The Modes I and II stress intensity factors at, for example, the crack tip $x_1 = a$ are defined by

$$k_1(a) = \lim_{x_1 \to a} \sqrt{2(x_1-a)}\, \sigma_{22}(x_1,0) ,$$

$$k_2(a) = \lim_{x_1 \to a} \sqrt{2(x_1-a)}\, \sigma_{12}(x_1,0) . \qquad (28)$$

Observing that equations (26) give the stress components $\sigma_{22}(x_1,0)$ and $\sigma_{12}(x_1,0)$ on the plane of the crack for $|x_1| > a$ as well as $|x_1| < 0$, substituting from (27) into (26) a simple asymptotic analysis would show that

$$\sigma_{22}(x_1,0) = \frac{Em_1}{\delta}\left[\frac{F_1(-a)}{\sqrt{2a(-x_1-a)}} - \frac{F_1(a)}{\sqrt{2a(x_1-a)}} + O(\sqrt{x_1^2-a^2})\right] ,$$

$$\sigma_{12}(x_1,0) = Em_2\delta\left[\frac{F_2(-a)}{\sqrt{2a(-x_1-a)}} - \frac{F_2(a)}{\sqrt{2a(x_1-a)}} + O(\sqrt{x_1^2-a^2})\right]. \qquad (29)$$

Thus, from (28) and (29) we obtain

$$k_1(-a) = \frac{Em_1}{\delta\sqrt{a}} F_1(-a) , \quad k_1(a) = -\frac{Em_1}{\delta\sqrt{a}} F_1(a) ,$$

$$k_2(-a) = \frac{Em_2\delta}{\sqrt{a}} F_2(-a) , \quad k_2(a) = -\frac{Em_2\delta}{\sqrt{a}} F_2(a) . \qquad (30)$$

From (22), (27), and (30) the crack opening displacements in the neighborhood of the crack tip, for example, $x_1 = a$ may be expressed as follows:

$$u_2(x_1,+0)-u_2(x_1,-0) = \frac{\delta k_1(a)}{Em_1}\sqrt{2(a-x_1)} + O((a-x_1)^{3/2}) ,$$

$$u_1(x_1,+0)-u_1(x_1,-0) = \frac{k_2(a)}{\delta Em_2}\sqrt{2(a-x_1)} + O((a-x_1)^{3/2}) . \qquad (31)$$

If U is the work done by the external forces and V is the internal potential, for a crack extension da the crack closure energy may be expressed as

$$d(U-V) = \int_a^{a+da} \frac{1}{2}\{\sigma_{22}(x_1,0)[u_2(x_1-da,+0) - u_2(x_1-da,-0)]$$

$$+ \sigma_{12}(x_1,0)[u_1(x_1-da,+0) - u_1(x_1-da,-)]\}dx_1 . \qquad (32)$$

From (31) and (32) the rate of internally released or externally added energy (for the extension of the crack at one tip) may then be expressed as follows:

$$G = \frac{d}{da}(U-V) = \frac{\pi}{4E}\left(\frac{\delta k_1^2}{m_1} + \frac{k_2^2}{\delta m_2}\right) . \qquad (33)$$

In the isotropic materials $\delta = 1$, $\kappa = 1$, $m_1 = m_2 = 1/4$, and for the plane stress case under consideration G becomes

$$G = \frac{\pi}{E}(k_1^2 + k_2^2) . \qquad (34)$$

4. Collinar Cracks

In formulating the problem, aside from the stress continuity conditions (19) no conditions of symmetry were assumed with regard to the crack geometry and the external loads $\sigma(x_1)$ and $\tau(x_1)$. Thus, the integral equations (26) derived in Section 2 are valid basically for any

number of collinear cracks defined by $x_2 = 0$, $a_j < x_1 < b_j$, $(j=1,\ldots,n)$ along the x_1 axis with the additional single-valuedness conditions of the form (23) for each crack, namely

$$\int_{a_j}^{b_j} G_{jk}(x_1)dx_1 = 0 \ , \ (k=1,2;\ j=1,\ldots,n) \ . \tag{35}$$

The only change in the integral equations would be in replacing the interval $(-a,a)$ by the sum of the intervals $L_i = (a_i,b_i)$ $(i=1,\ldots,n)$ corresponding to the collinear cracks.

As an example, we consider the case of two symmetrically located and symmetrically loaded collinear cracks. That is, we assume that $a_1=a$, $b_1=b$, $a_2=-b$, $b_2=-a$, $H_1=H_2=H$, $\sigma_{12}(x_1,0) = \tau(x_1) = \tau(-x_1)$, $\sigma_{22}(x_1,0) = \sigma(x_1) = \sigma(-x_1)$, $(a < x_1 < b)$. In this case, referring to (26) it may be shown that for the loading conditions $\sigma(x_1) \neq 0$, $\tau(x_1) = 0$ and $\sigma(x_1) = 0$, $\tau(x_1) \neq 0$ the integral equations uncouple and, by using the symmetry conditions, may be expressed as

$$\frac{1}{\pi}\int_a^b [\frac{1}{t_1-x_1} + \frac{1}{t_1+x_1} + K_{11}(x_1,t_1)]G_1(t_1)dt_1 = \frac{\delta}{Em_1}\sigma(x_1), \ a<x_1<b \ , \tag{36}$$

$$\frac{1}{\pi}\int_a^b [\frac{1}{t_1-x_1} + \frac{1}{t_1+x_1} + K_{22}(x_1,t_1)]G_2(t_1)dt_1 = \frac{1}{Em_2\delta}\tau(x_1), \ a<x_1<b, \tag{37}$$

where

$$K_{11}(x_1,t_1) = k_{11}(x_1,t_1) - k_{11}(x_1,-t_1) \ ,$$

$$K_{22}(x_1,t_1) = k_{22}(x_1,t_1) - k_{22}(x_1,-t_1) \ , \ a < (x_1,t_1) < b \ . \tag{38}$$

The integral equations (36) and (37) are again solved under the following single-valuedness conditions:

$$\int_a^b G_1(t_1)dt_1 = 0 \quad , \quad \int_a^b G_2(t_1)dt_1 = 0 \quad . \tag{39}$$

In this problem the unknown functions G_1 and G_2 are of the form

$$G_1(x_1) = \frac{F_1(x_1)}{\sqrt{(b-x_1)(x_1-a)}} \, , \; G_2(x_1) = \frac{F_2(x_1)}{\sqrt{(b-x_1)(x_1-a)}} \, , \tag{40}$$

and the stress intensity factors may be obtained from

$$k_1(a) = \frac{Em_1}{\delta} \lim_{x_1 \to a} \sqrt{2(x_1-a)}\, G_1(x_1) \, ,$$

$$k_2(a) = Em_2\delta \lim_{x_1 \to a} \sqrt{2(x_1-a)}\, G_2(x_1) \, ,$$

$$k_1(b) = -\frac{Em_1}{\delta} \lim_{x_1 \to b} \sqrt{2(b-x_1)}\, G_1(x_1) \, ,$$

$$k_2(b) = -Em_2\delta \lim_{x_1 \to b} \sqrt{2(b-x_1)}\, G_2(x_1) \, . \tag{41}$$

5. Loading the Strip by a Rigid Wedge

Consider now the problem described in Figures 1(b) and (c). It is assumed that an orthotropic strip containing a symmetrically located crack is loaded by a rigid frictionless rectangular wedge of thickness v_0. Because of symmetry $\sigma_{12}(x_1,0) = 0, (-\infty<x_1<\infty)$, $G_2(x_1) = 0$, $(-a<x_1<a)$, $k_{12}(x_1,t_1) = 0 = k_{21}(x_1,t_1)$, $(-a<(x_1,t_1)<a)$, the second equation in (26) is identically satisfied, and assuming that the contact is maintained along the entire length of the wedge $-b<x_1<b$, the first integral equation may be expressed as

$$\frac{1}{\pi} \int_{-a}^{a} \left[\frac{1}{t_1-x_1} + k_{11}(x_1,t_1)\right] G_1(t_1)dt_1 = \frac{\delta}{Em_1}\sigma(x_1), \; -a<x_1<a \, . \tag{42}$$

We now note that for the continuous contact problem shown in Fig. 1(b)

$$G_1(x_1) = 0,\ -b<x_1<b,\ \sigma(x_1) = 0,\ b<|x_1|<a\ , \tag{43}$$

and (42) may be expressed as

$$\frac{1}{\pi}\int_{-a}^{-b}\left[\frac{1}{t_1-x_1} + k_{11}(x_1,t_1)\right]G_1(t_1)dt_1 + \frac{1}{\pi}\int_{b}^{a}\left[\frac{1}{t_1-x_1} + k_{11}(x_1,t_1)\right]G_1(t_1)dt_1 = 0$$

$$b<|x_1|<a\ . \tag{44}$$

By referring to the collinear crack problem described in the previous section and by using the conditions of symmetry in loading and geometry the integral equation (44) may be simplified as follows:

$$\frac{1}{\pi}\int_{b}^{a}\left[\frac{1}{t_1-x_1} + \frac{1}{t_1+x_1} + K_{11}(x_1,t_1)\right]G_1(t_1)dt_1 = 0,\ b<x_1<a\ . \tag{45}$$

Equation (45) must be solved under loading condition

$$\int_{b}^{a} G_1(t_1)dt_1 = -v_0\ . \tag{46}$$

Since the wedge has "sharp" corners in this case, too, the solution of (45) has square root singularities at the end points a and b and may be expressed as

$$G_1(x_1) = \frac{F_1(x_1)}{\sqrt{(a-x_1)(x_1-b)}},\ (b<x_1<a) \tag{47}$$

where F_1 is a bounded function.

Intuitively, it is clear that the continuous contact described above is valid only for relatively short wedges, as b/a increases separation may occur in the center portion of the wedge. This problem may

be investigated and the critical ratio of b/a for initiation of separation may be determined by calculating the contact pressure along $x_2 = 0$, $-b<x_1<b$, and by calculating the value of b/a at which this pressure becomes zero (presumably at $x_1 = 0$). It must be emphasized that $(b/a)_{cr}$ would be independent of the wedge thickness v_0. In (45) and (46) dividing the equations by v_0 it is seen that G_1/v_0 may be determined uniquely. Thus, v_0 enters into the expression of the contact pressure simply as a multiplying factor and would have no effect on its relative distribution. Once $G_1(x_1)$ is determined the contact stress may be obtained from

$$\sigma_{22}(x_1,0) = \frac{Em_1}{\pi\delta}\int_b^a [\frac{1}{t_1-x_1} + \frac{1}{t_1+x_1} + K_{11}(x_1,t_1)]G_1(t)dt_1, \quad 0<x_1<b. \tag{47}$$

For $(b/a) > (b/a)_{cr}$ the separation would take place along $-c<x_1<c$, $x_2=0$. In this case by defining

$$G_1(x_1) = g_1(x_1), \quad b<|x_1|<a, \quad G_1(x_1) = g_2(x_1), \quad -c<x_1<c \ , \tag{48}$$

and again by observing that

$$G_1(x_1) = 0, \quad |x_1|>a, \quad c<|x_1|<b \ ,$$

$$\sigma(x_1) = 0, \quad -c<x_1<c, \quad b<|x_1|<a \ , \tag{49}$$

the integral equations of the problem may be expressed as

$$\int_b^a [\frac{1}{t_1-x_1} + \frac{1}{t_1+x_1} + K_{11}(x_1,t_1)]g_1(t_1)dt_1 + \int_{-c}^{c} [\frac{1}{t_1-x_1} + k_{11}(x_1,t_1)]g_2(t_1)dt_1$$

$$= 0, \quad b<x_1<a \ , \tag{50}$$

$$\int_{-c}^{c}\left[\frac{1}{t_1-x_1}+k_{11}(x_1,t_1)\right]g_2(t_1)dt_1+\int_{b}^{a}\left[\frac{1}{t_1-x_1}+\frac{1}{t_1+x_1}\right.$$

$$\left.+K_{11}(x_1,t_1)\right]g_1(t_1)dt_1=0\ ,\ -c<x_1<c\ , \qquad (51)$$

Note that in (50) and (51) only the first integrals have singular kernels. Also note that at $x_1 = \mp c$ the contact is "smooth". Thus, the solution of (50) and (51) is of the following form:

$$g_1(x_1)=\frac{f_1(x_1)}{\sqrt{(a-x_1)(x_1-b)}}\ ,\ g_2(x_1)=f_2(x_1)\sqrt{c^2-x_1^2} \qquad (52)$$

where f_1 and f_2 are (unknown) bounded functions having the symmetry properties $f_i(x_1) = -f_i(-x_1)$, $(i=1,2)$. The loading for the homogeneous system (50) and (51) is again provided by

$$\int_{b}^{a}g_1(t_1)dt_1=-v_o\ . \qquad (53)$$

In this case, too, the contact stress, indeed the stress component $\sigma_{22}(x_1,0)$ may be calculated from (50) or (51) by observing that these expressions give $\sigma_{22}(x_1,0)$ outside as well as the inside the cracks.

6. Results

In the general problem the system of integral equations (26) is solved for loading conditions $\sigma(x_1) \neq 0$, $\tau(x_1) = 0$ and $\sigma(x_1) = 0$, $\tau(x_1) \neq 0$ separately. In doing so there is no need for specifying the stiffness parameter $\delta = (E_{11}/E_{22})^{1/4}$ explicitly as δ enters into the expressions of the kernels k_{ij} through $H\delta/a$ only. Thus, if $\tau(x_1) = 0$ one may solve for G_1/δ and G_2 from (26) and obtain $F_1(\mp a)/\delta$ and $F_2(\mp a)$ for given values of H_1/H_2, $H\delta/a$, and κ. Equations (30) would then give k_1 and k_2/δ, and

k_2 may be obtained after specifying δ. The important point to make here is that decreasing δ for constant H/a has the same magnifying effect on the Mode I stress intensity factor k_1 as decreasing the ratio H/a for constant δ. Similarly, if $\sigma(x_1) = 0$, $\tau(x_1) \neq 0$ (26) may be solved for G_1 and $G_2\delta$ for given κ, $\delta H/a$, and H_1/H_2, and (30) would give k_2 and $k_1\delta$. In this case, too, decreasing δ would have the same magnifying effect on k_2 as decreasing H/a. The second important observation to be made is that in the uncoupled problem, i.e., for $H_1=H_2=H$ the stress intensity factors k_1 and k_2 depend on δ through $H\delta/a$ only. Therefore, in most of the results given in this paper, the stiffness ratio δ is not explicitly specified.

The results for a single crack are given in Figures 2-6 and Tables 1-4. Figures 2 and 3 show the effect of the crack location H_1/H on the stress intensity factors in a uniformly loaded specific orthotropic material, namely yellow birch, and in an isotropic strip. As expected, for $(H_1/H) \to 0$, k_1 and k_2 become unbounded. A somewhat unexpected result here is that in the case of shear loading as H_1/H decreases k_2 does not monotonously increase, it rather goes through a minimum before becoming unbounded (Fig. 3). Figures 4 and 5 show the effect of H/a on the stress intensity factors in an isotropic strip ($\delta=\kappa=1$) and in orthotropic strips having the properties $\kappa=1$, $\delta=1/3$ or $\kappa=1$, $\delta=3$. Note that this covers a range of $1/81<E_{11}/E_{22}<81$ for the stiffness ratio. For constant shear parameter κ the effect of $H\delta/a$ on the stress intensity factors is shown in Fig. 6.

Further results for an orthotropic strip containing a single crack are given in Tables 1-4. Table 1 shows the stress intensity factors for a concentrated wedge loading (see, for example, the insert in Fig. 10). The effect of H/a on the stress intensity factors in an isotropic and in two specific orthotropic strips containing a symmetric crack under various loading conditions is shown in Table 2. The effect of shear parameter κ is shown in Table 3 and that of δ (for a given thickness ratio H/a = 0.35) is shown in Table 4. It is seen that compared to

the influence of δ the effect of κ on the stress intensity factors is negligible.

A sample result for two pressurized collinear cracks in an orthotropic strip is shown in Fig. 7 which also shows the stress intensity factors in the corresponding infinite plane (i.e., for $H/(b-a)/2 = \infty$) obtained from (see, for example, [11])

$$k_1(b) = p\sqrt{(b-a)/2}\,\left(\frac{2}{1-a/b}\right)^{1/2}\,\left[1 - \frac{E(k)}{K(k)}\right]/k\ ,$$

$$k_1(a) = p\sqrt{(b-a)/2}\,\left(\frac{2}{\frac{a}{b}(1-\frac{a}{b})}\right)^{1/2}\,\left[\frac{E(k)}{K(k)} - \left(\frac{a}{b}\right)^2\right]/k\ , \qquad (54)$$

where $k = \sqrt{1-a^2/b^2}$ and $K(k)$ and $E(k)$ are the complete elliptic integrals of the first and second kind, respectively. Tables 5-7 show further results. In these examples the half crack length $(b-a)/2$ is used as the normalizing length parameter. $a/b = 0$ and $a/b = 1$ correspond to two limiting cases of a single crack of length $2b$ and $b-a$, respectively. Perhaps the most interesting result here is the fact that for small values of $H\delta/(b-a)/2$ k_1 (particularly $k_1(a)$) goes through a minimum as a/b goes from zero to 1. This reduction is apparently due to the interaction of the stress fields developing around the two cracks. For example, as seen from Figures 8-10 the cleavage stress $\sigma_{22}(x_1,0)$ in the plane of the crack, even though tensile and unbounded in the close neighborhood of the crack tip, becomes compressive in a certain interval away from the crack tip. This is essentially due to the "bending" effect of the two halves of the strip. This effect diminishes and disappears as the thickness ratio H/a increases. No such behavior is observed for strips under shear loading.

Fig. 7 and Tables 5-7 show that for $a\to 0$ as expected $k_i(a)$, $(i=1,2)$, becomes unbounded, whereas $k_i(b)$ tends to the values corresponding to a single crack of length $2b$. It may be observed that the rate of increase of $k_i(b)$ $(i=1,2)$ as (a/b) approaches zero is very high. In fact, the derivative of $k_i(b)$ at $a/b = 0$ may be shown to be infinite.

For example, noting that for small values of a/b

$$K(k) = \log\left(\frac{4}{a/b}\right) + \frac{1}{4}\left[\log\left(\frac{4}{a/b}\right)-1\right](a/b)^2 + \ldots ,$$

$$E(k) = 1 + \frac{1}{2}\left[\log\left(\frac{4}{a/b}\right) - \frac{1}{2}\right](a/b)^2 + \ldots , \qquad (55)$$

from (54) it can be shown that

$$\frac{d}{d(a/b)}\, k_1(b) \tilde{=} - p\sqrt{b}\, \frac{1}{\frac{a}{b}\left[\log \frac{a}{b}\right]^2} \qquad (56)$$

which becomes unbounded at a/b = 0.

The results for the orthotropic strip loaded by a rectangular rigid wedge of thickness v_0 are shown in Figures 11-14 and Tables 8 and 9. For κ=2 and $H\delta/a$ = 0.6 the contact stress distribution $\sigma_{22}(x_1,0) = -p(x)$, $(x=x_1/a)$ corresponding to b/a ratios greater than, equal to, and smaller than $(b/a)_{cr}$ is given in Fig. 11, where $(b/a)_{cr}$ corresponds to the initiation of interface separation. It is seen that for the case of continuous contact (e.g., b/a = 0.2) the pressure is minimum at x_1=0 where it becomes "negative" for $(b/a) > (b/a)_{cr}$. In the case of $b > b_{cr}$ the contact stress is of the following form

$$\sigma_{22}(x_1,0) = -p(x_1/a) = h(x_1)\sqrt{\frac{x_1-c}{b-x_1}}\,, \quad c<x_1<b\,, \qquad (57)$$

where $h(x_1)$ is a bounded function. The calculated length 2c of the separation zone is shown in Fig. 12. Critical wedge length b_{cr} corresponding to κ=2 and various values of $H\delta/a$ is given in Table 8. The table also shows the normalized crack tip stress intensity factor $k_1(a) = k_{1A}$ and the stress intensity factor for the contact stress at x_1=b defined by (see (57))

$$k_{1B} = k_1(b) = \lim_{x_1\to b} \sqrt{b-x_1}\ \sigma_{22}(x_1,0)\ . \qquad (58)$$

Table 9 shows k_{1A} and k_{1B} for the case of continuous contact, i.e., for $b<b_{cr}$. Additional results for the separation case are given in Figures 13 and 14. In these figures the starting points of the graphs correspond to $(b/a)_{cr}$.

References

1. S. Krenk, Int. J. Solids Structures, Vol. 11 (1975), 449.

2. D.D. Ang and M.L. Williams, Journal of Applied Mechanics, Vol. 28, Trans. ASME (1961), 372.

3. G.C. Sih, P.C. Paris, G.R. Irwin, International Journal of Fracture Mechanics, Vol. 1 (1965), 189.

4. F. Delale and F.Erodgan, Journal of Applied Mechanics, Vol. 44, Trans. ASME (1977), 237.

5. A.C. Kaya and F. Erdogan, International Journal of Fracture, Vol. 16 (1980), 171.

6. F. Delale, I. Bakirtas, and F. Erdogan, Journal of Applied Mechanics, Vol. 46, Trans. ASME (1979), 90.

7. S.G. Lekhnitskii, Theory of Elasticity of an Anisotropic Elastic Body, Holden-Day Inc. (1963).

8. S. Krenk, Journal of Composite Materials, Vol. 13 (1979), 108.

9. A. Cinar, The Crack and Crack-Contact Problems for an Orthotropic Strip, M.S. Thesis, Lehigh University, (1980).

10. F. Erdogan, Mechanics Today, Vol. 4, S. Nemat-Nasser, ed., Pergamon, Oxford (1978), 1.

11. F. Erdogan, Proc. 4th U.S. National Congress of Applied Mechanics, ASME (1962), 547.

Table 1. Stress intensity factors in an orthotropic strip subjected to concentrated forces on the crack surfaces, $\sigma_{22}(x_1,0) = P\delta(x_1)$ $\sigma_{12}(x_1,0) = 0$, $\kappa = 1.2895$.

$\delta H/a$	$H_1=H_2=H$	$H_1=0.7H$		$H_1=0.4H$	
	$\frac{k_1}{(P/a)\sqrt{a}}$	$\frac{k_1}{(P/a)\sqrt{a}}$	$\frac{-k_2}{(P/a)\sqrt{a}}$	$\frac{k_1}{(P/a)\sqrt{a}}$	$\frac{-k_2}{(P/a)\sqrt{a}}$
1.5	0.613	0.681	0.104	1.061	0.353
1.0	0.880	1.008	0.207	1.638	0.700
0.6	1.517	1.767	0.472	3.038	1.555
0.4	2.470	2.895	0.869	5.164	2.875
0.25	4.514	5.344	1.777	9.872	5.864
0.15	9.091	10.822	3.859	17.866	11.193
0.10	16.177	19.098	7.069		

Table 2. Stress intensity factors in isotropic and orthotropic strips which contain a symmetrically located crack (i.e., $H_1=H_2=H$) subjected to various loading conditions.

	$\sigma_{22}(x_1,0)=-p$			$\sigma_{22}(x_1,0)=P\delta(x_1)$			$\sigma_{12}(x_1,0)=-q$		
	$k_1/p\sqrt{a}$			$k_1/(P/a)\sqrt{a}$			$k_2/q\sqrt{a}$		
H/a	$\kappa=1=\delta$	$\kappa=2=\delta$	$\kappa=2,\ \delta=1/2$	$\kappa=1=\delta$	$\kappa=2=\delta$	$\kappa=2,\ \delta=1/2$	$\kappa=1=\delta$	$\kappa=2=\delta$	$\kappa=2,\ \delta=1/2$
0.2	9.376	4.047		6.249	2.403		2.629	1.789	
0.4	4.146	2.175	8.865	2.511	1.133	5.811	1.934	1.391	2.405
0.6	2.758	1.655	5.509	1.536	0.774	3.421	1.640	1.238	2.015
0.8	2.149	1.422	4.047	1.128	0.612	2.403	1.473	1.159	1.789
1.0	1.816	1.294	3.248	0.892	0.524	1.849	1.365	1.113	1.640
1.2	1.611	1.216	2.751	0.745	0.470	1.508	1.289	1.084	1.533
1.6	1.377	1.130	2.175	0.581	0.411	1.133	1.192	1.051	1.391
3.0	1.122	1.040	1.466	0.404	0.351	0.643	1.067	1.016	1.175

Table 3: The effect of the shear parameter κ on the stress intensity factors.

(a) $\frac{H_1}{H} = 1.0$, $\frac{\delta H}{a} = 0.35$

κ	$\sigma(x_1)=p$, $\tau(x_1)=0$	$\sigma(x_1)=P\delta(x_1)$, $\tau(x_1)=0$	$\sigma(x_1)=0$, $\tau(x_1)=q$
	$k_{1A}=k_{1B}$	$k_{1A}=k_{1B}$	$k_{2A}=k_{2B}$
	$\frac{k_{1B}}{p\sqrt{a}}$	$\frac{k_{1B}}{(P/a)\sqrt{a}}$	$\frac{k_{2B}}{q\sqrt{a}}$
1	4.801	2.971	2.047
2	4.657	2.826	1.890
4	4.564	2.697	1.717
8	4.553	2.612	1.550
12	4.611	2.592	1.463
16	4.692	2.613	1.405

(b) $\frac{H_1}{H} = 0.4$, $\frac{\delta H}{a} = 0.35$

κ	$\sigma(x_1)=p$, $\tau(x_1)=0$		$\sigma(x_1)=P\delta(x_1)$, $\tau(x_1)=0$		$\sigma(x_1)=0$, $\tau(x_1)=q$	
	$k_{1A}=k_{1B}$	$k_{2A}=-k_{2B}$	$k_{1A}=k_{1B}$	$k_{2A}=-k_{2B}$	$k_{1A}=-k_{1B}$	$k_{2A}=k_{2B}$
	$\frac{k_{1B}}{p\sqrt{a}}$	$\frac{k_{2B}}{\delta p\sqrt{a}}$	$\frac{k_{1B}}{(P/a)\sqrt{a}}$	$\frac{k_{2B}}{\delta(P/a)\sqrt{a}}$	$\frac{\delta k_{1B}}{q\sqrt{a}}$	$\frac{k_{2B}}{q\sqrt{a}}$
1	9.519	-4.855	6.342	-3.646	0.846	1.658
2	8.986	-4.404	5.903	-3.295	0.761	1.553
4	8.447	-3.908	5.432	-2.905	0.666	1.441
8	7.968	-3.370	4.977	-2.487	0.563	1.336
12	7.753	-3.095	4.737	-2.266	0.508	1.283

Table 4. Effect of the stiffness parameter δ on the stress intensity factors, $\frac{H_1}{a} = \frac{H_2}{a} = 0.35$, $\kappa = 2$.

δ	$\sigma_{22}(x_1,0)=p$	$\sigma_{22}(x_1,0)=P\delta(x_1)$	$\sigma_{12}(x_1,0)=q$
	$\frac{k_{1B}}{p\sqrt{a}}$	$\frac{k_{1B}}{(P/a)\sqrt{a}}$	$\frac{k_{2B}}{q\sqrt{a}}$
0.3	20.350	14.218	3.231
0.4	13.880	9.426	2.829
0.6	8.348	5.436	2.353
0.8	5.954	3.732	2.075
1.2	3.851	2.261	1.755
1.5	3.103	1.745	1.610
1.8	2.637	1.427	1.507
2	2.415	1.279	1.453
3	1.797	0.858	1.282
10	1.112	0.393	1.043

Table 5. Stress intensity factors in an orthotropic strip containing two identical collinear cracks loaded by uniform crack surface pressure p or shear q; $H_1=H_2=H$, $\kappa=1$, $H\delta/(b-a)/2 = 0.4$.

$\frac{2a}{b-a}$	$\sigma_{22}(x_1,0)=-p$		$\sigma_{12}(x_1,0)=-q$	
	$\frac{k_1(b)}{p(\frac{b-a}{2})^{1/2}}$	$\frac{k_1(a)}{p(\frac{b-a}{2})^{1/2}}$	$\frac{k_2(b)}{q(\frac{b-a}{2})^{1/2}}$	$\frac{k_2(a)}{q(\frac{b-a}{2})^{1/2}}$
0	9.376	∞	2.629	∞
.01	3.693	6.996	2.106	5.837
.1	3.788	2.837	1.952	2.300
.2	3.962	3.113	1.935	1.989
.3	4.074	3.642	1.933	1.939
.4	4.124	3.971	1.933	1.933
.5	4.138	4.103	1.933	1.932
.6	4.141	4.138	1.933	1.933
.7	4.140	4.143	1.933	1.933
.8	4.140	4.142	1.933	1.933
.9	4.139	4.140	1.933	1.933
1	4.139	4.140	1.933	1.933
2	4.142	4.142	1.933	1.933

Table 6. Stress intensity factors in an orthotropic strip containing two identical collinear cracks loaded by uniform crack surface pressure p or shear q; $\kappa=2$, $H\delta/(b-a)/2 = 0.4$.

$\frac{2a}{b-a}$	$\sigma_{22}(x_1,0)=-p$		$\sigma_{22}(x_1,0)=-q$	
	$\frac{k_1(b)}{p(\frac{b-a}{2})^{1/2}}$	$\frac{k_1(a)}{p(\frac{b-a}{2})^{1/2}}$	$\frac{k_2(b)}{q(\frac{b-a}{2})^{1/2}}$	$\frac{k_2(a)}{q(\frac{b-a}{2})^{1/2}}$
0	8.865	∞	2.405	∞
.01	3.626	7.023	1.993	5.657
.1	3.697	2.890	1.825	2.252
.2	3.847	3.126	1.799	1.908
.3	3.950	3.547	1.792	1.824
.4	4.004	3.814	1.790	1.800
.5	4.028	3.947	1.790	1.793
.6	4.039	4.005	1.790	1.790
.7	4.044	4.030	1.789	1.790
.8	4.045	4.040	1.789	1.790
.9	4.046	4.044	1.789	1.789
1	4.046	4.046	1.789	1.789
2	4.047	4.047	1.789	1.789

Table 7. Stress intensity factors in an orthotropic strip containing two identical collinear cracks loaded by uniform crack surface pressure p or shear q; $\kappa=2$, $H\delta/(b-a)/2 = 0.8$.

$\frac{2a}{b-a}$	$\sigma_{22}(x_1,0)=-p$		$\sigma_{12}(x_1,0)=-q$	
	$\frac{k_1(b)}{p(\frac{b-a}{2})^{1/2}}$	$\frac{k_1(a)}{p(\frac{b-a}{2})^{1/2}}$	$\frac{k_2(b)}{q(\frac{b-a}{2})^{1/2}}$	$\frac{k_2(a)}{q(\frac{b-a}{2})^{1/2}}$
0	4.047	∞	1.789	∞
.01	2.207	6.843	1.677	4.951
.1	2.012	2.448	1.482	2.057
.2	2.017	1.999	1.433	1.676
.3	2.046	1.913	1.412	1.532
.4	2.079	1.931	1.402	1.464
.5	2.106	1.981	1.397	1.430
.6	2.127	2.033	1.394	1.412
.7	2.143	2.075	1.393	1.402
.8	2.154	2.107	1.392	1.397
.9	2.161	2.130	1.391	1.394
1	2.166	2.146	1.391	1.393
2	2.174	2.174	1.391	1.391
3	2.175	2.175	1.391	1.391

Table 8. The critical values of $\frac{b}{a}$ for various values of $\delta H/a$, shear parameter $\kappa = 2$.

$\frac{\delta H}{a}$	$(\frac{b}{a})_{cr}$	$\frac{\delta a}{Ev_o} \frac{k_{1A}}{\sqrt{a}}$	$\frac{\delta a}{Ev_o} \frac{k_{1B}}{\sqrt{a}}$
1.5	0.961	4.761×10^{-1}	-4.568×10^{-1}
1.0	0.665	1.569×10^{-1}	-1.476×10^{-1}
0.60	0.293	8.544×10^{-2}	-6.792×10^{-2}
0.40	0.161	5.836×10^{-2}	-3.874×10^{-2}
0.20	0.059	2.801×10^{-2}	-1.188×10^{-2}

Table 9. Stress intensity factors in an orthotropic strip loaded by a rectangular wedge for $(b/a) < (b/a)_{cr}$ (Fig. 1b), $\kappa=2$, $k_o = Ev_o\sqrt{a}/(a\delta)$ (underlined values correspond to initiation of separation at $x_1 = 0$).

b/a	$H\delta/a=1$		$H\delta/a=1.5$	
	k_{1A}/k_o	$-k_{1B}/k_o$	k_{1A}/k_1	$-k_{1B}/k_o$
0.2	0.0932	0.0858		
0.3			0.104	0.109
0.4	0.113	0.0983		
0.6	0.143	0.132	0.146	0.139
<u>0.665</u>	<u>0.157</u>	<u>0.148</u>		
0.8			0.207	0.201
<u>0.961</u>			<u>0.475</u>	<u>0.455</u>

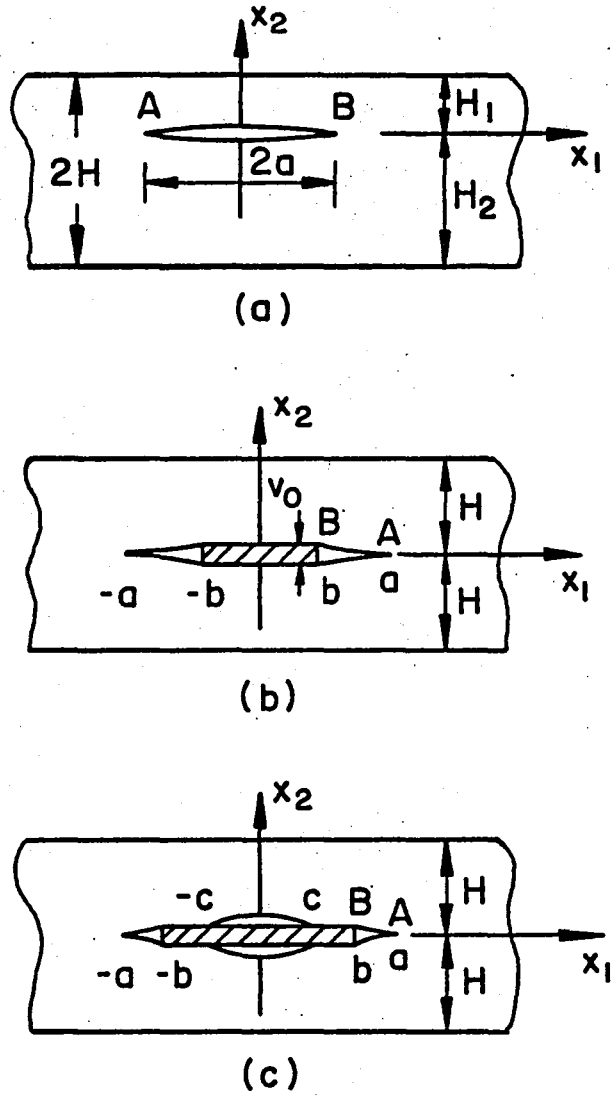

Figure 1: Geometry of the crack and crack-contact problems.

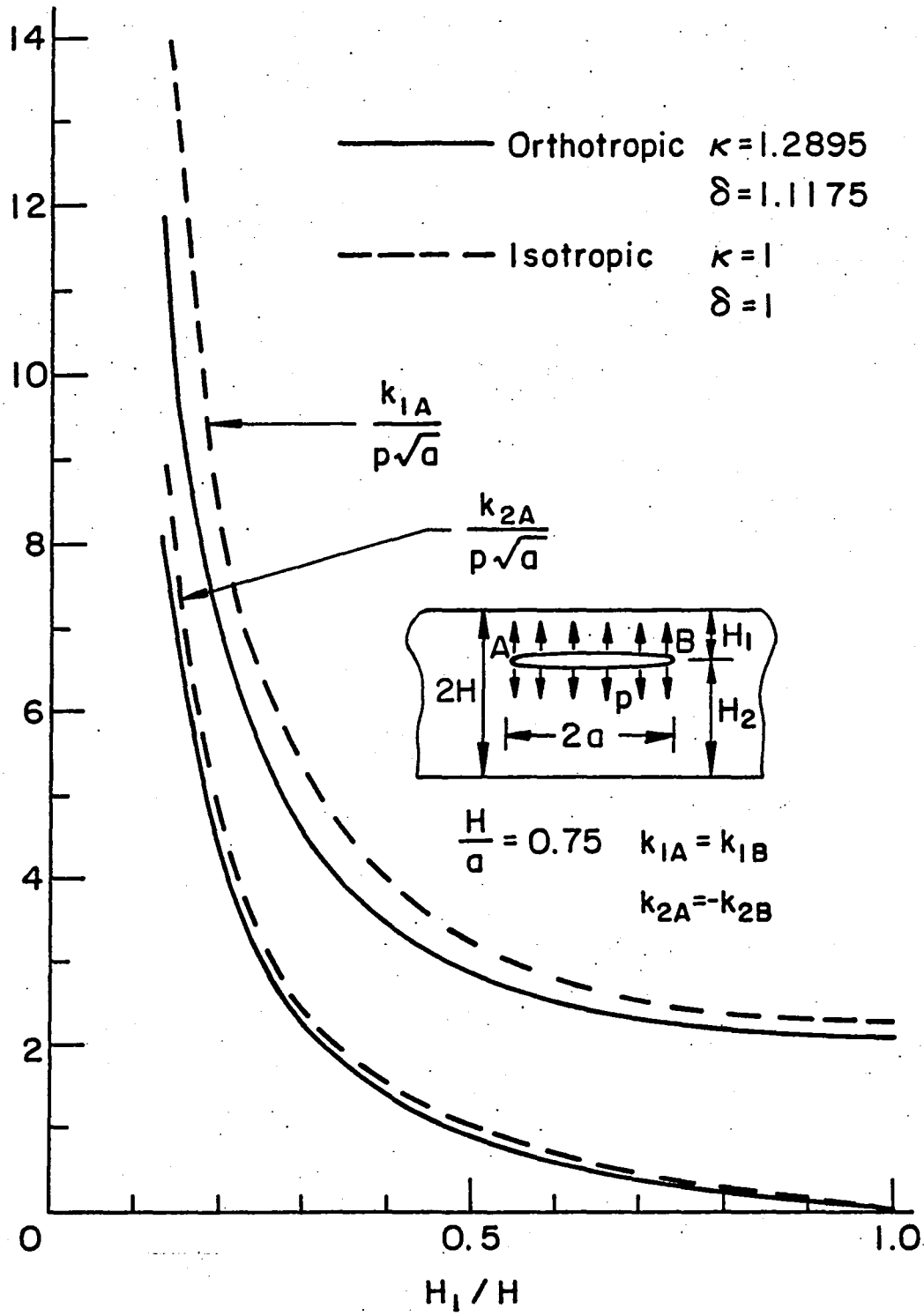

Figure 2: The effect of the crack location on the stress intensity factors for uniform surface pressure. H = 0.75a, $\delta = 1 = \kappa$ for the isotropic materials and $\delta = 1.1175$, $\kappa = 1.2895$ for the orthotropic material (yellow birch).

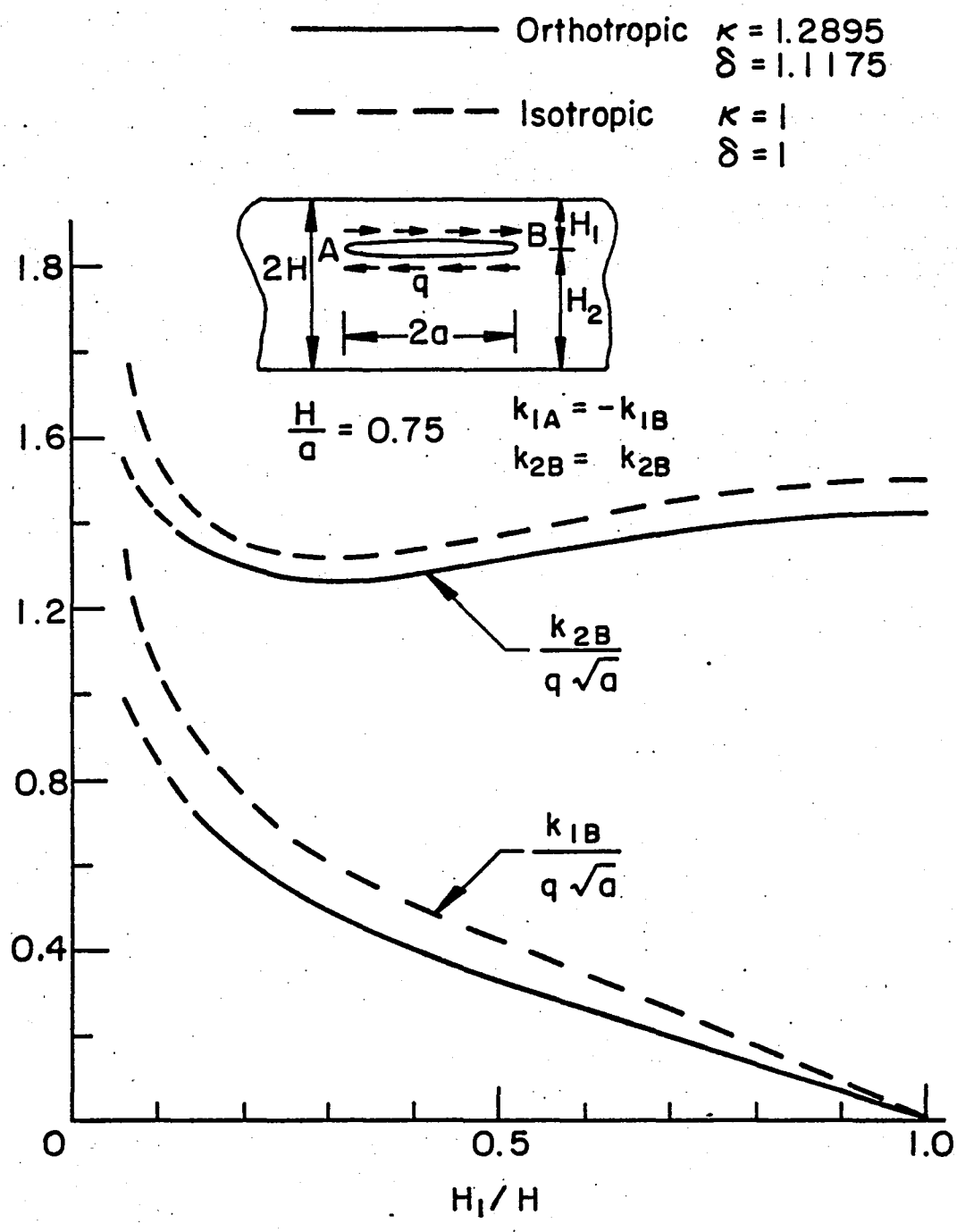

Figure 3: Same as figure 2 for uniform shear applied to the crack surface.

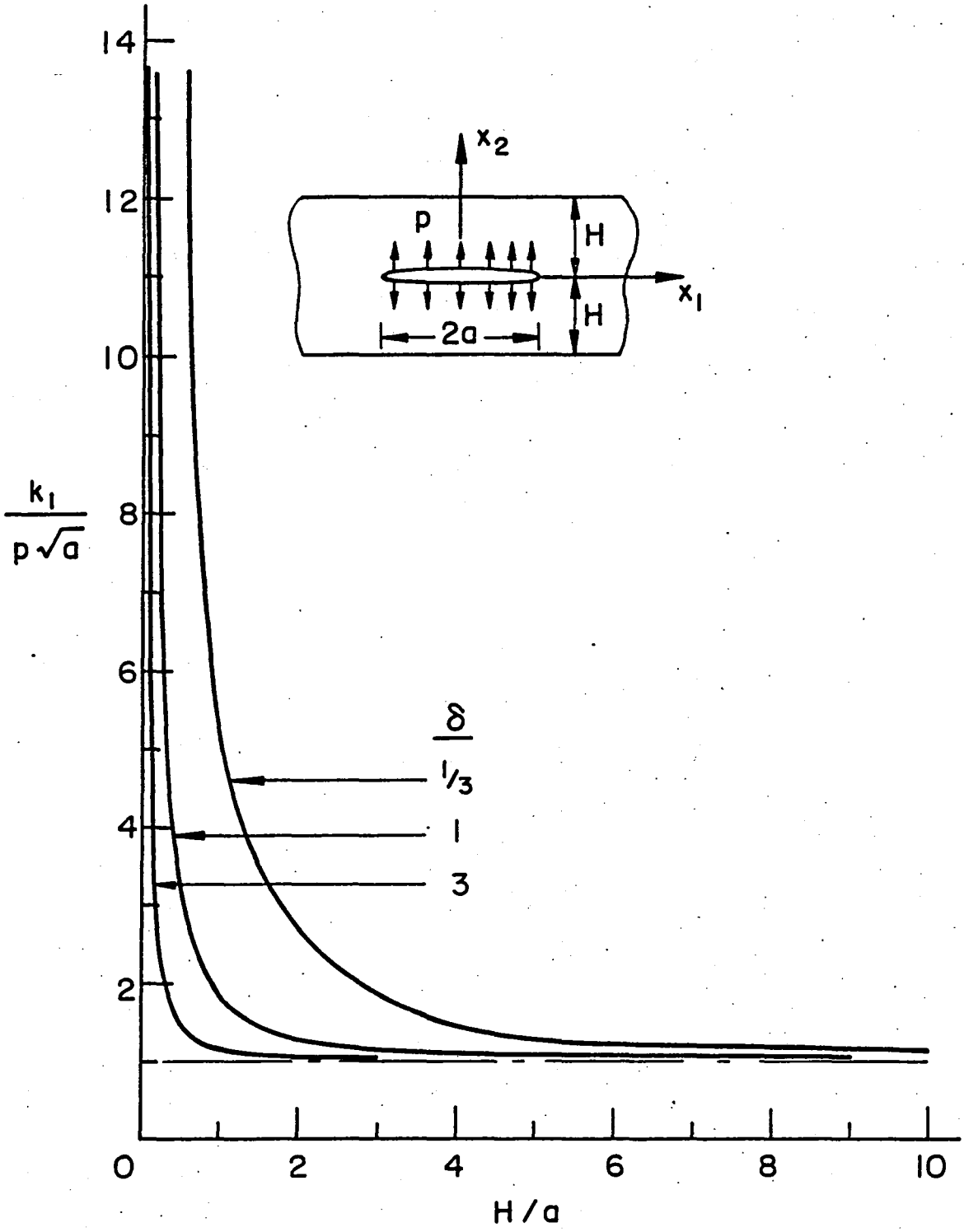

Figure 4: Effect of the crack length on the stress intensity factor for a symmetrically located crack under uniform pressure, $\kappa = 1$.

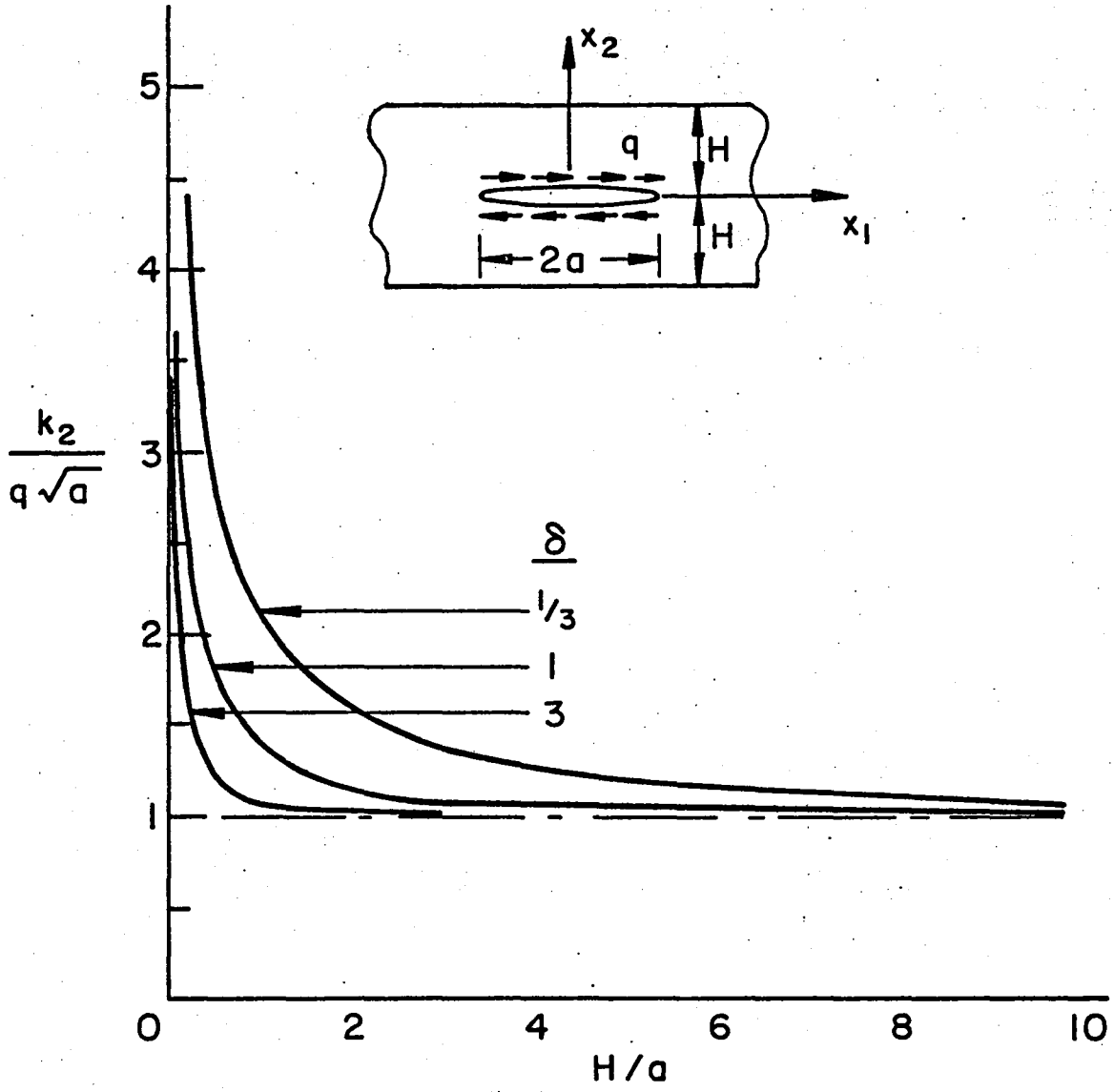

Figure 5: Same as figure 4 for uniform shear applied to crack surface.

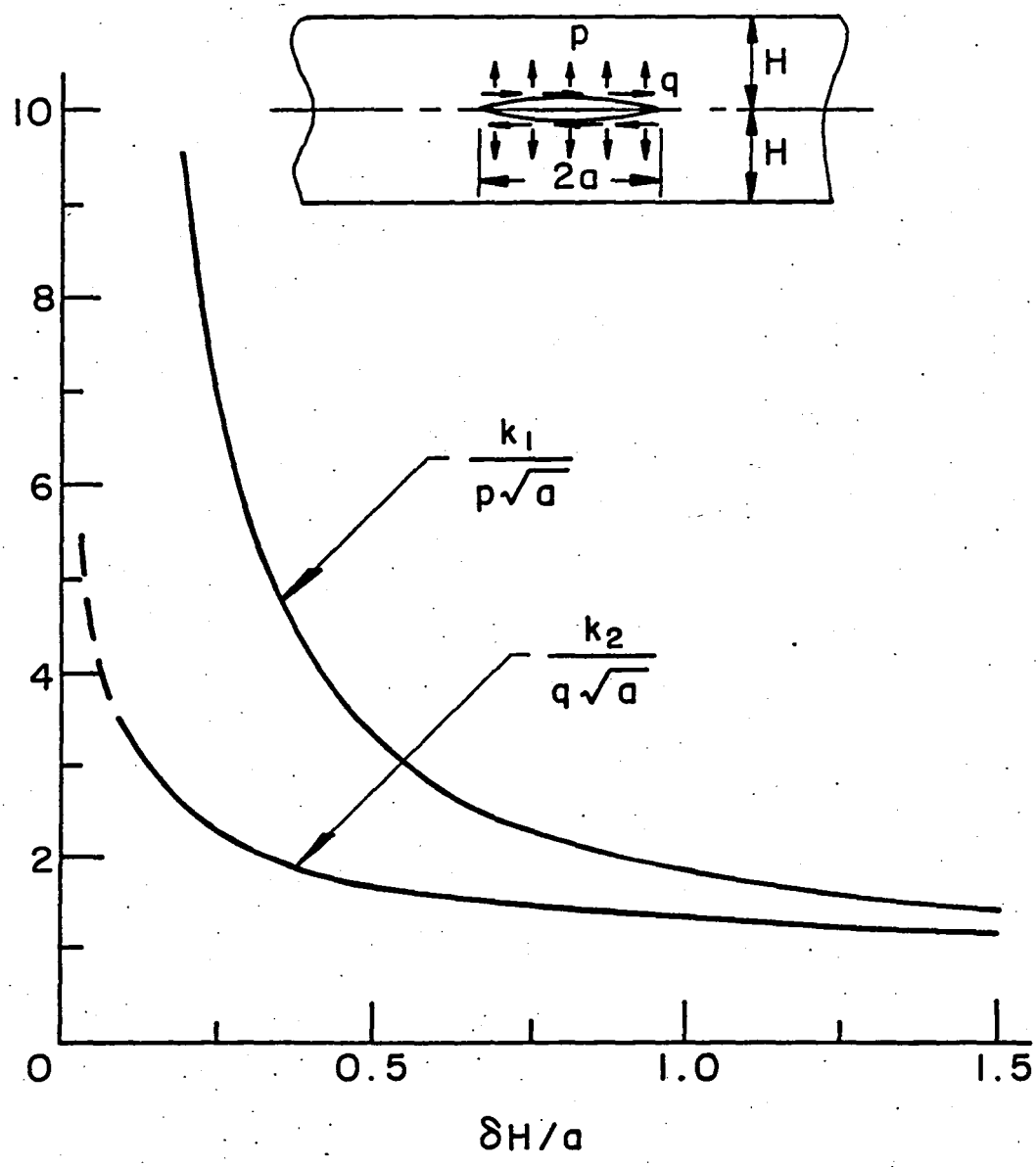

Figure 6: The effect of δH/a on the stress intensity factors for a symmetrically located crack under uniform pressure or uniform shear, $\kappa = 1.2895$.

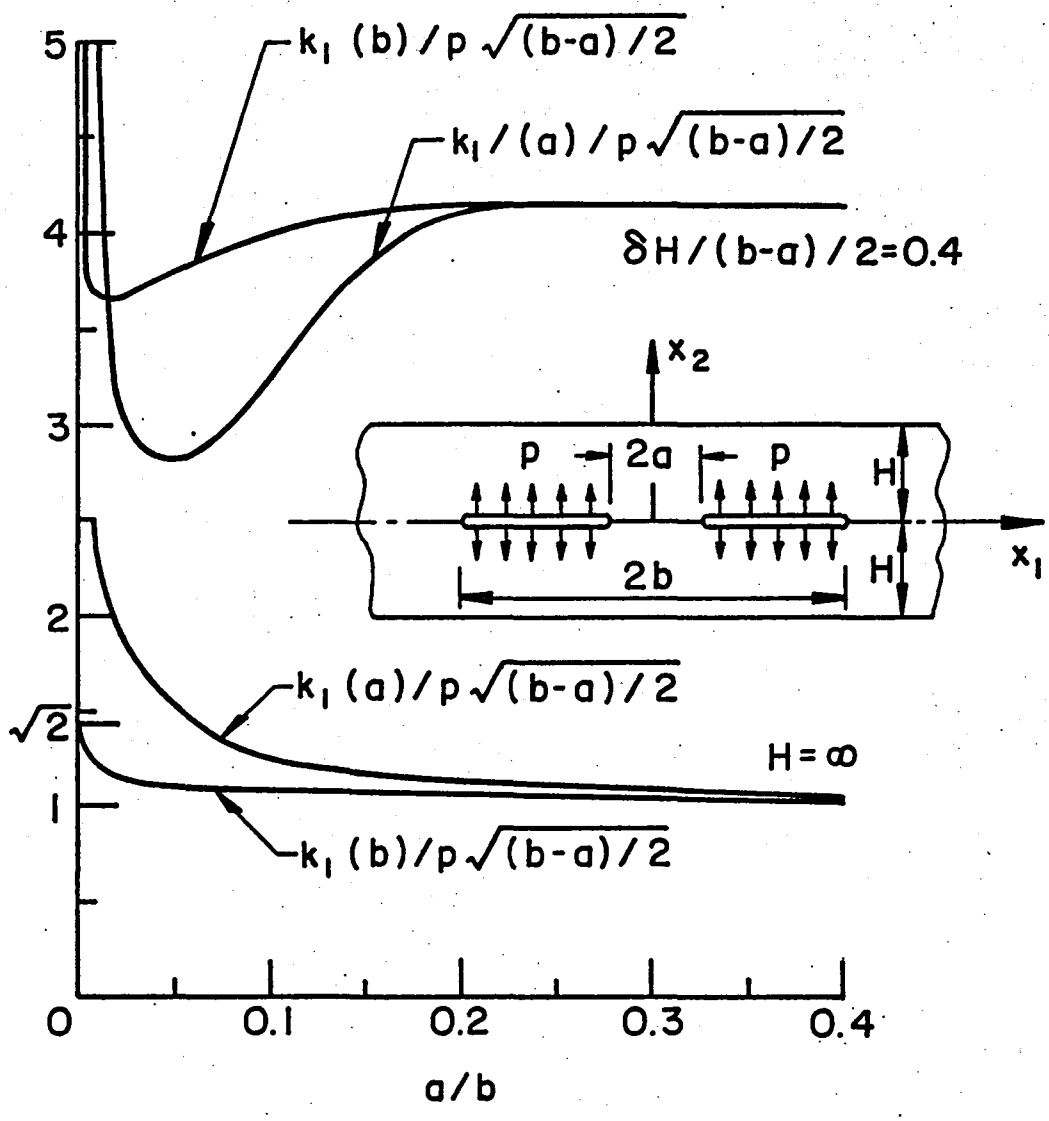

Figure 7. Stress intensity factors for two collinear cracks in an orthotropic strip.

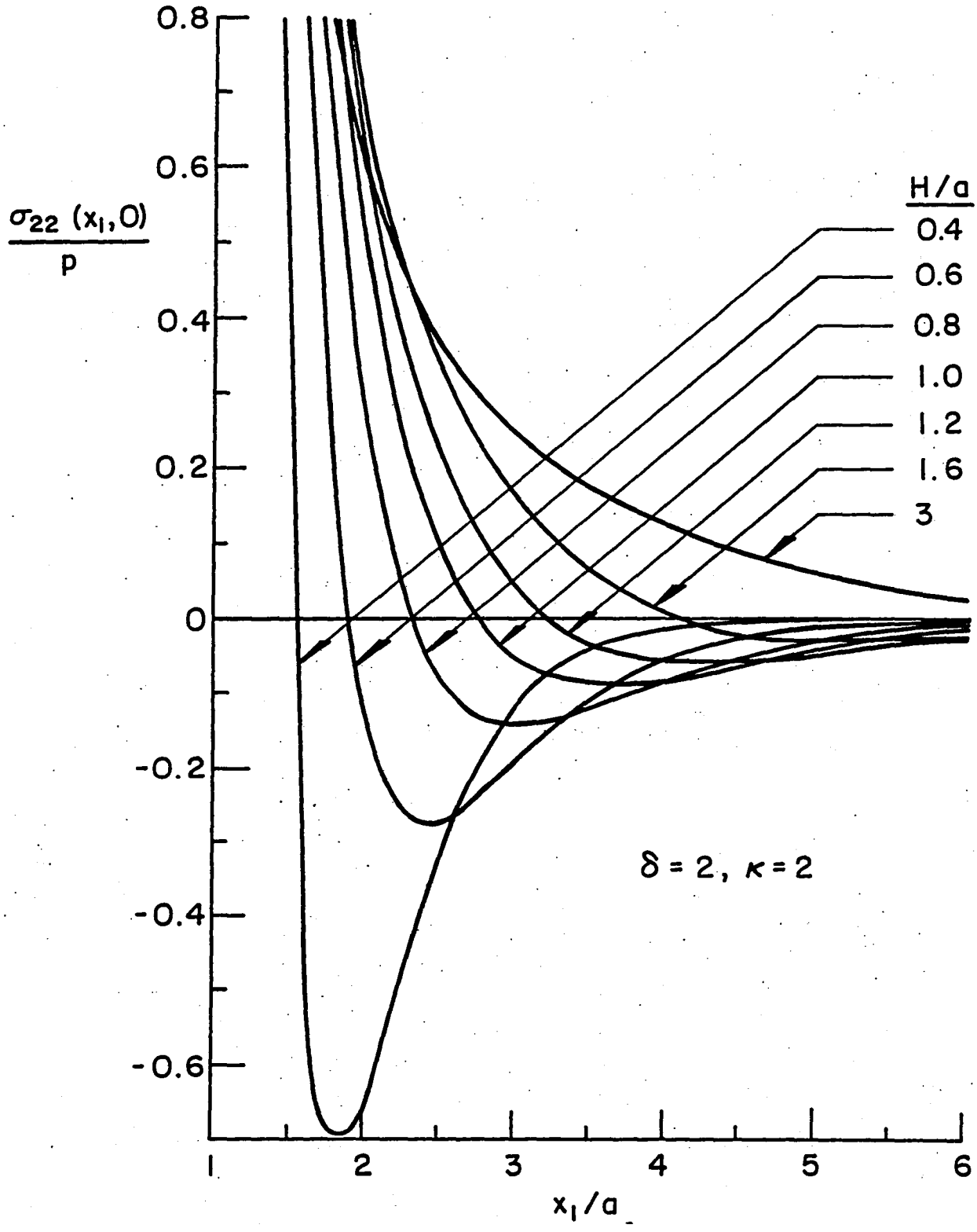

Figure 8. The effect of the relative crack size on the normal stress σ_{22} in the plane of the crack in an orthotropic strip containing a pressurized crack (see the insert in Fig. 9 for notation).

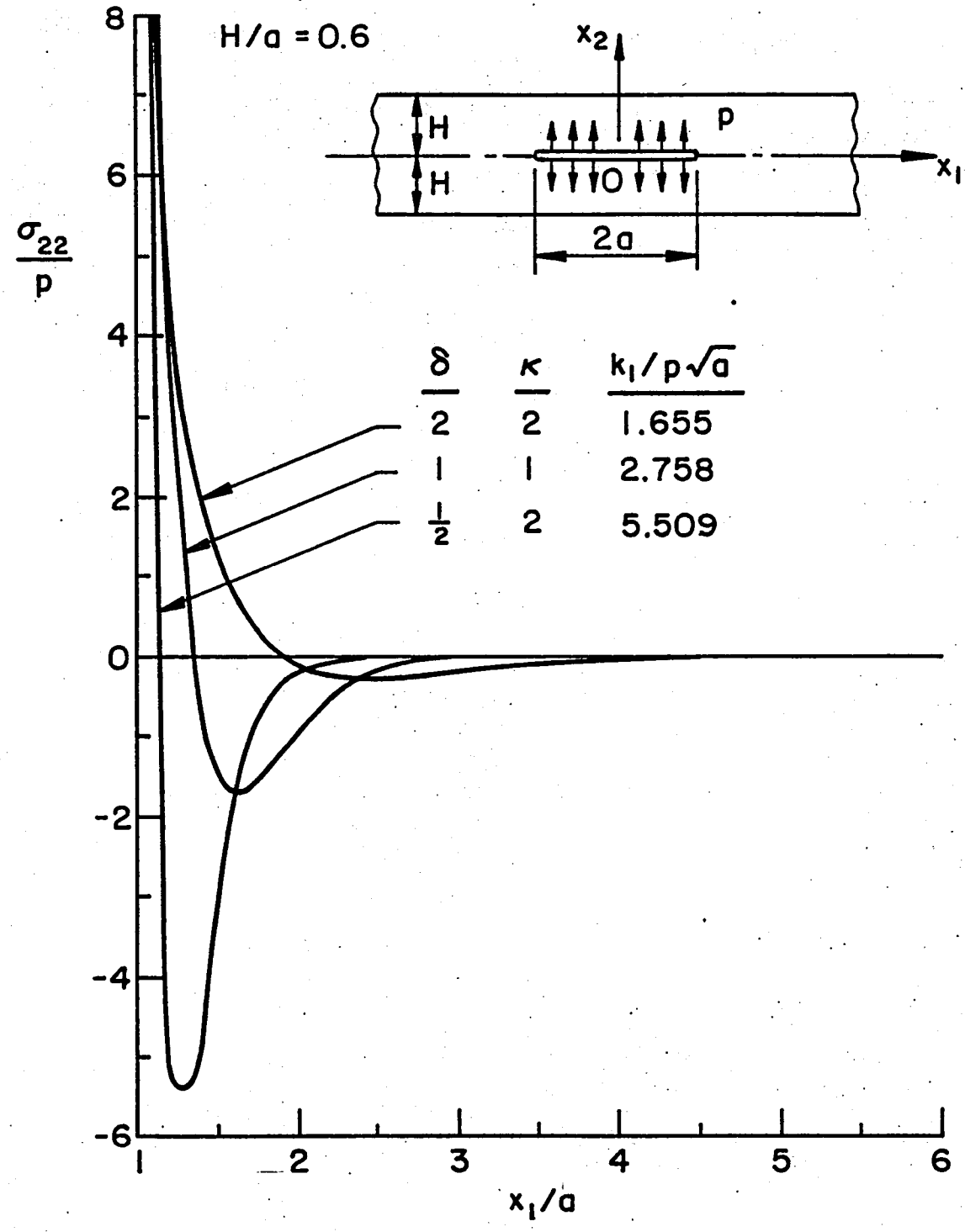

Figure 9. The effect of material orthotropy on the normal stress $\sigma_{22}(x_1,0)$ in a strip containing a pressurized crack ($\delta=\kappa=1$ isotropic strip).

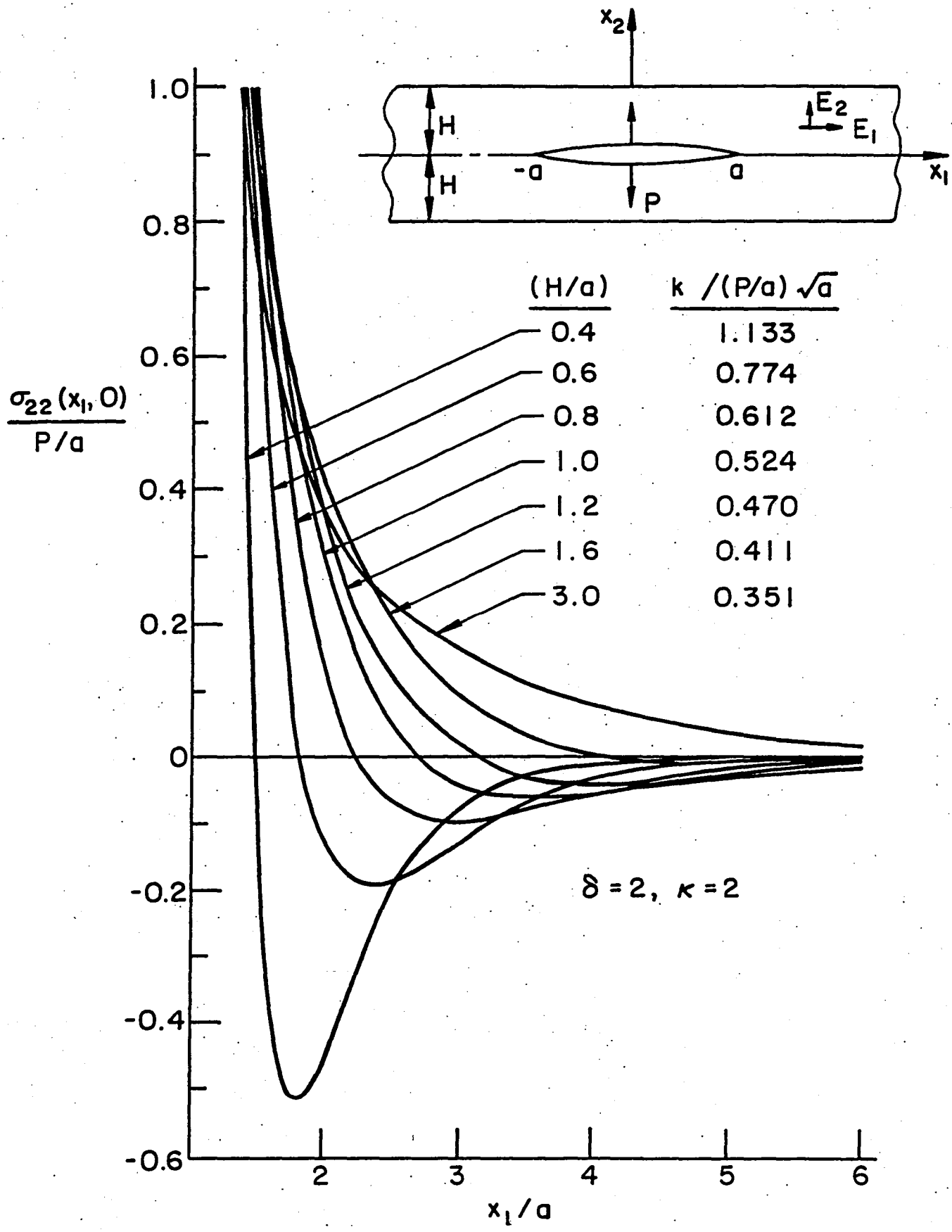

Figure 10. Same as Figure 8 in a cracked strip under concentrated wedge loading.

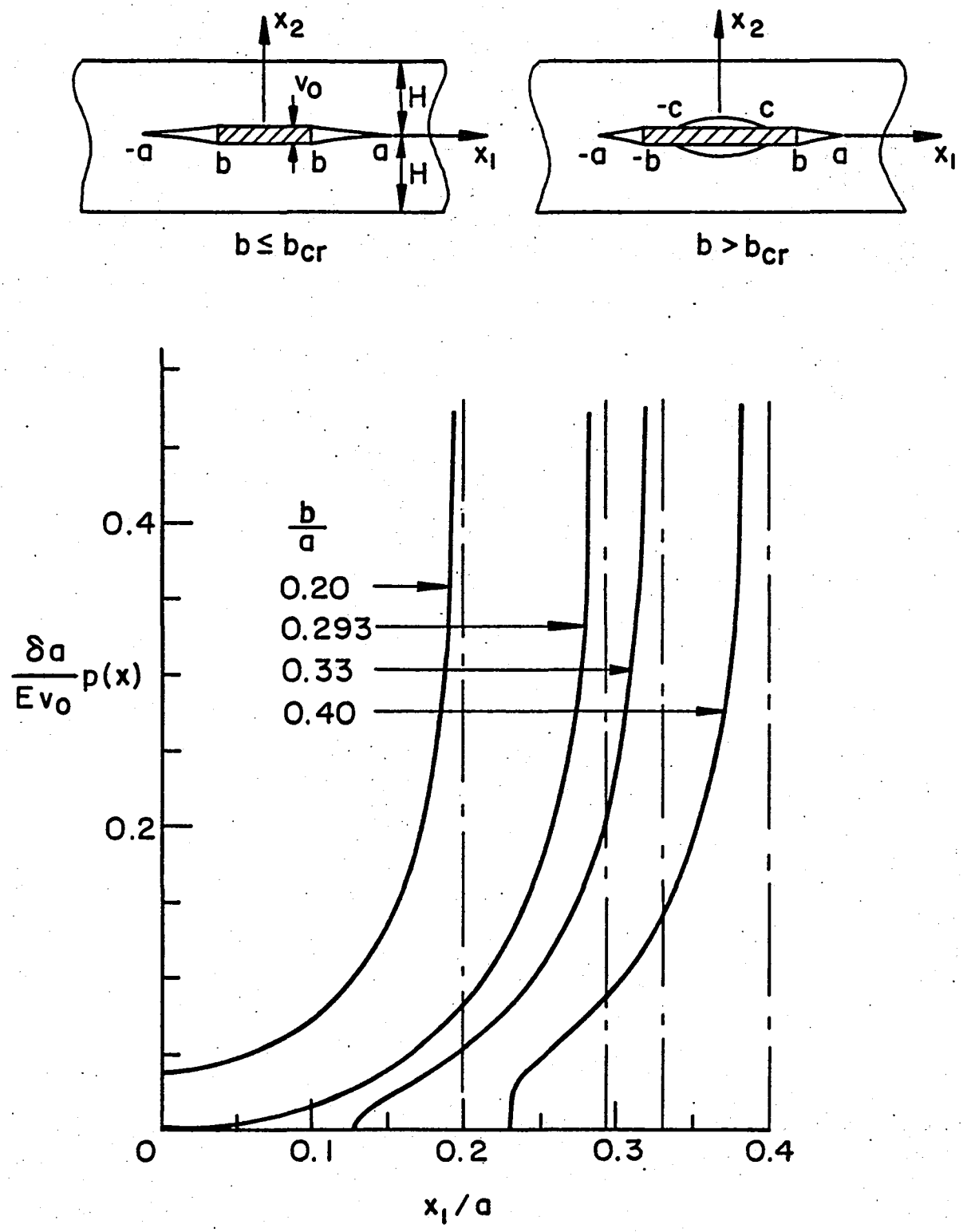

Figure 11. Pressure distribution for the wedge problem, $\delta H = 0.6a$, $\kappa=2$, $p(x) = -\sigma_{22}(x_1,0)$, $x=x_1/a$.

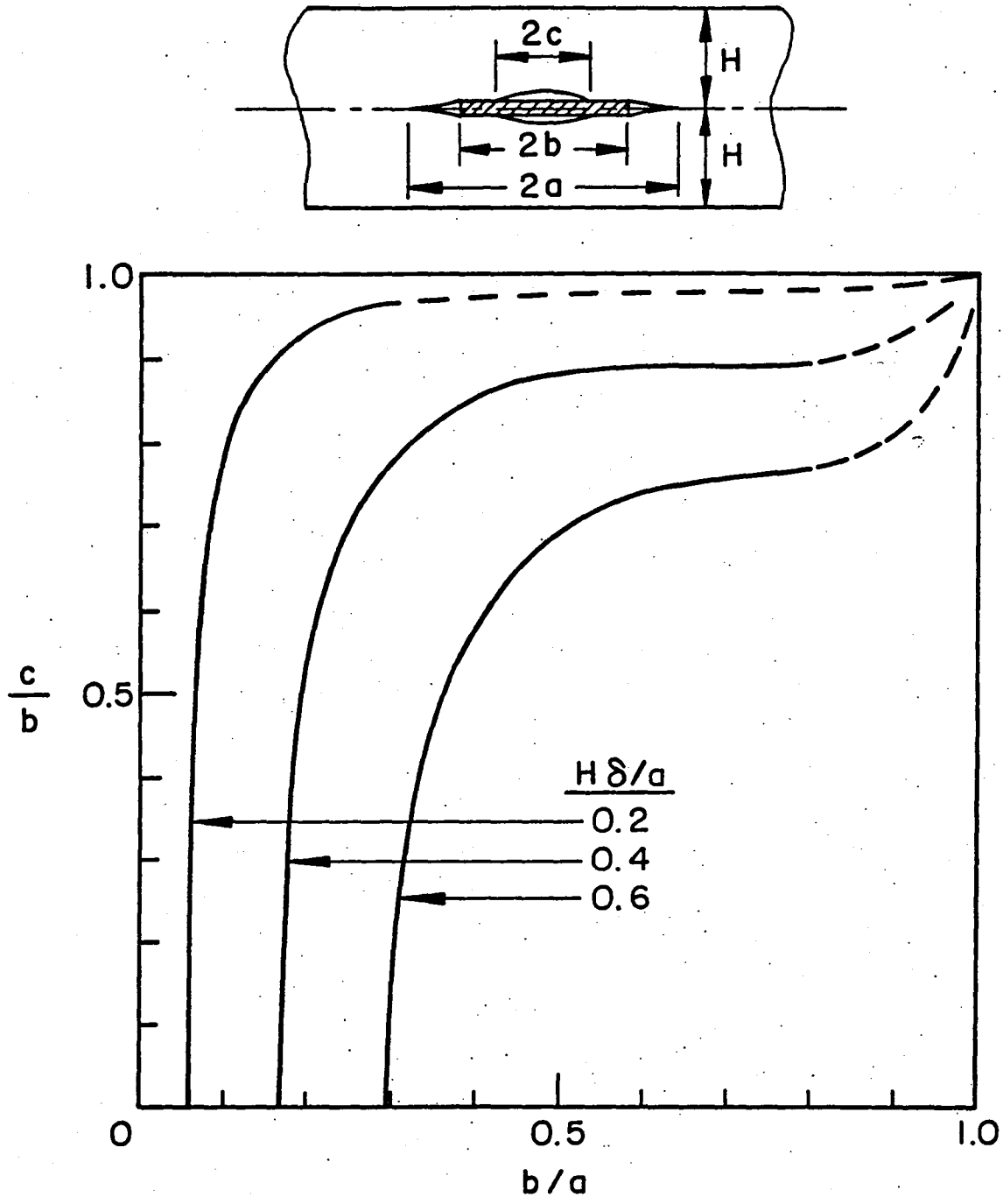

Figure 12: Separation length for the wedge problem, $\kappa = 2$.

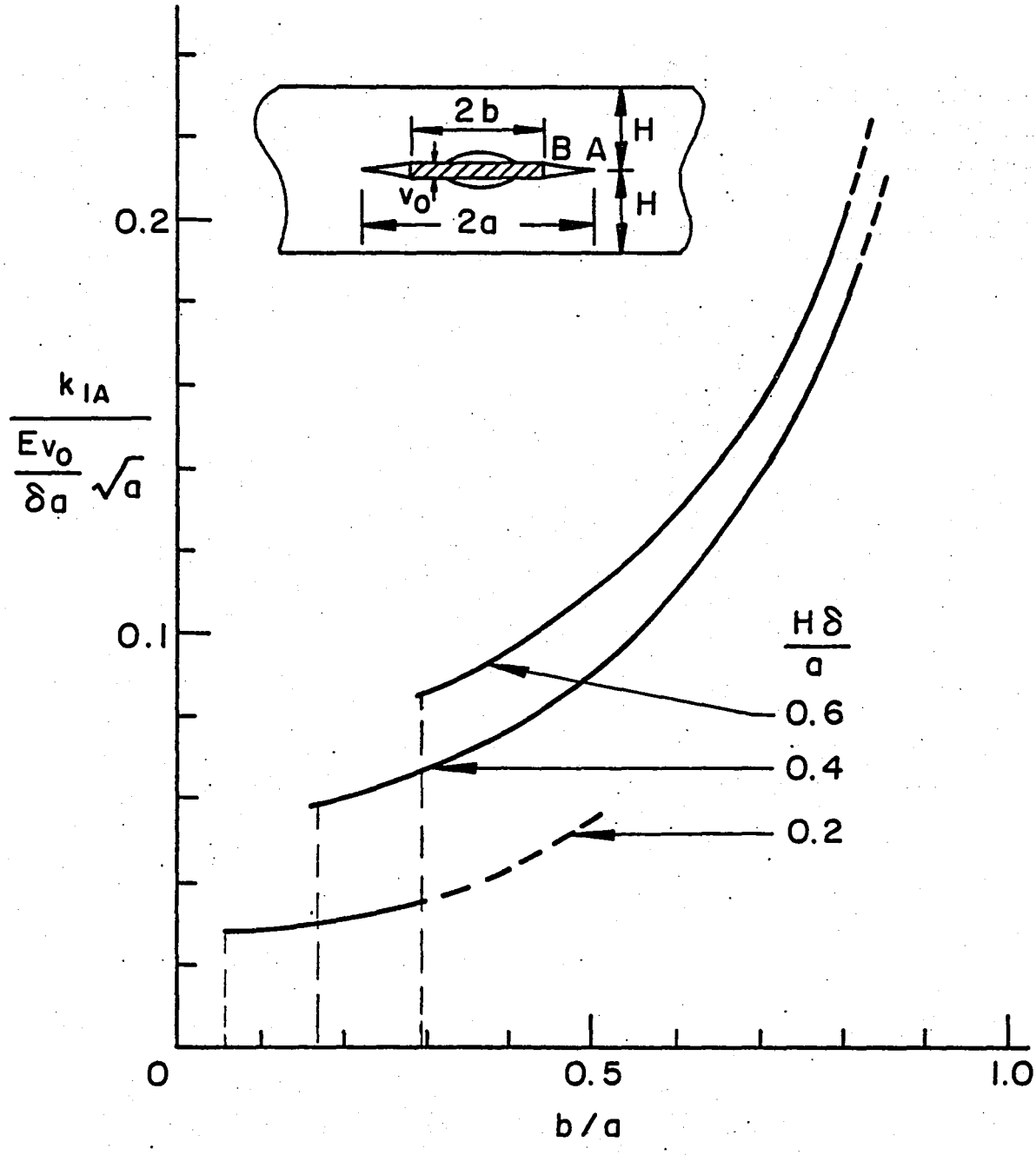

Figure 13: Crack tip stress intensity factor for the wedge problem, $\kappa = 2$.

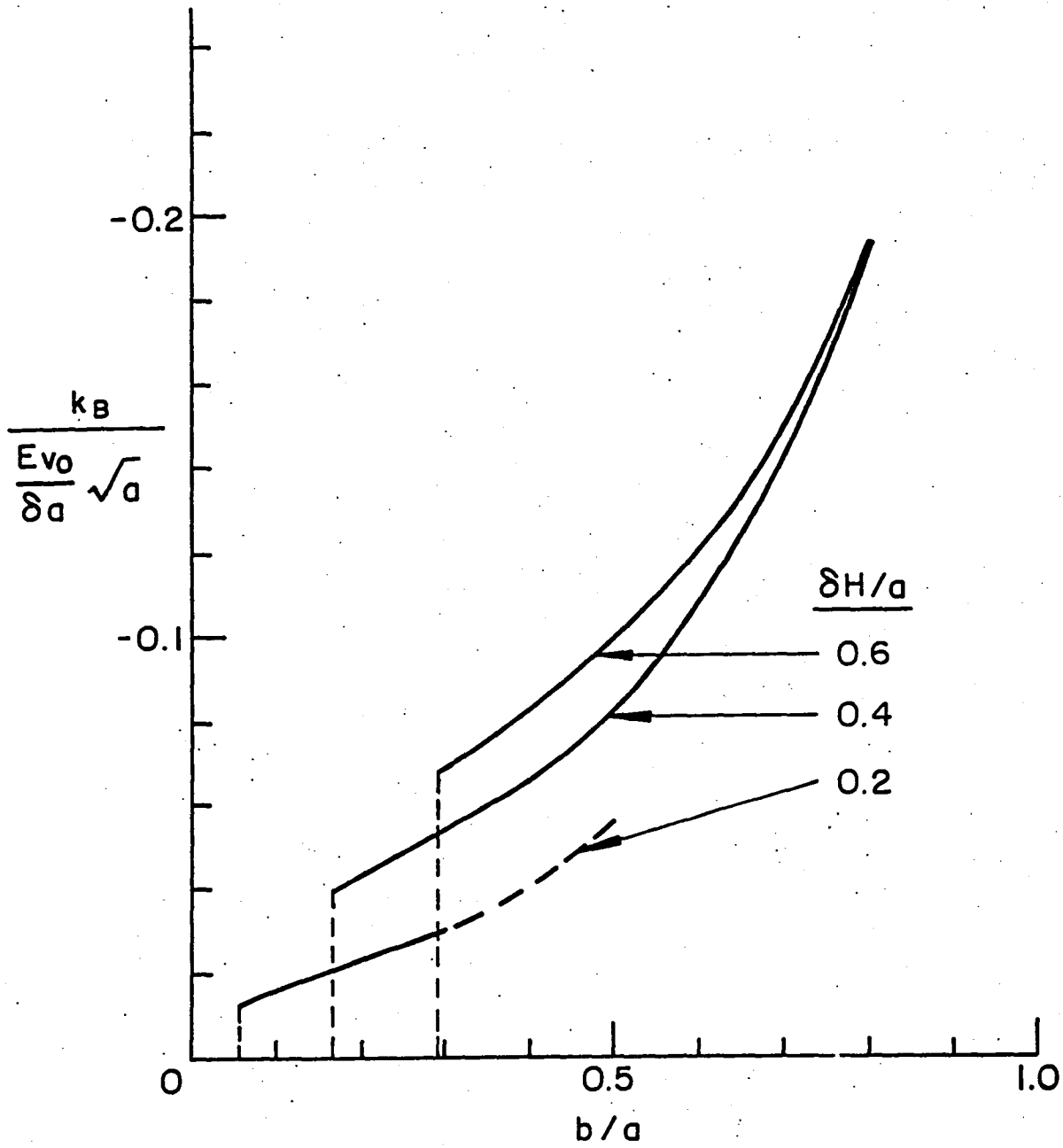

Figure 14: Wedge tip stress intensity factor for the crack contact problem, $\kappa = 2$.

1. Report No.	2. Government Accession No.	3. Recipient's Catalog No.
NASA CR-165990		

4. Title and Subtitle	5. Report Date
THE CRACK AND WEDGING PROBLEM FOR AN ORTHOTROPIC STRIP	September 1982
	6. Performing Organization Code
7. Author(s)	8. Performing Organization Report No.
A. Cinar and F. Erdogan	
	10. Work Unit No.
9. Performing Organization Name and Address	
Lehigh University Bethlehem, PA 18015	11. Contract or Grant No. NGR 39-007-011
	13. Type of Report and Period Covered
12. Sponsoring Agency Name and Address	Contractor Report
National Aeronautics and Space Administration Washington, DC 20546	14. Sponsoring Agency Code

15. Supplementary Notes

Langley technical monitor: Dr. John H. Crews, Jr.

16. Abstract

In this paper, first the plane elasticity problem for an orthotropic strip containing a crack parallel to its boundaries is considered. The problem is formulated under general mixed-mode loading conditions. It is shown that the stress-intensity factors depend on two dimensionless orthotropic constants only. For the crack problem, the results are given for a single crack and two collinear cracks. The calculated results show that of the two orthotropic constants the influence of the stiffness ratio on the stress-intensity factors is much more significant than that of the shear parameter. The problem of loading the strip by a rigid rectangular wedge is then considered. It is found that for relatively small wedge lengths continuous contact is maintained along the wedge-strip interface, at a certain critical wedge length the separation starts at the midsection of the wedge, and the length of the separation zone increases rapidly with increasing wedge length.

17. Key Words (Suggested by Author(s))	18. Distribution Statement
Orthotropic strip Crack Wedge loading Stress-intensity factor	Unclassified - Unlimited Subject Category 39

19. Security Classif. (of this report)	20. Security Classif. (of this page)	21. No. of Pages	22. Price*
Unclassified	Unclassified	42	A03

* For sale by the National Technical Information Service, Springfield, Virginia 22161

End of Document